

Near-infrared time-series photometry of six fields in the young open cluster IC 2391

Chris Koen^{1,2★} and Akika Ishihara^{3,4}

¹*Department of Statistics, University of the Western Cape, Private Bag X17, Bellville, 7535 Cape, South Africa*

²*SAAO, PO Box 9, Observatory, 7935 Cape, South Africa*

³*Department of Earth and Planetary Science, University of Tokyo, 7-3-1 Hongo, Bunkyo, Tokyo 113-0033, Japan*

⁴*National Astronomical Observatory of Japan, 2-21-1 Osawa, Mitaka, Tokyo 181-8588, Japan*

Accepted 2006 March 15. Received 2006 March 15; in original form 2005 August 15

ABSTRACT

Fields containing targets of spectral types later than M5 were monitored in JHK_s for about 7 h each. None of the targets showed variability at levels exceeding 0.02 (or smaller, in some cases). Seven new variable stars were discovered serendipitously. The large number of measurements (more than 50) of each field allows the construction of accurate colour–magnitude and colour–colour diagrams. These could be used to identify a small number of candidate very cool objects.

Key words: stars: low-mass, brown dwarfs – stars: variables: other.

1 INTRODUCTION

At a distance of about 150 pc (Patten & Simon 1996; Dodd 2004) the open cluster IC 2391 is one of the closest to earth, and therefore one of the easiest to study. It is relatively young – a recent age estimate based on lithium depletion is ~ 53 Myr (Barrado y Navascués, Stauffer & Patten 1999), while other techniques suggest that the cluster may be even younger (~ 30 – 35 Myr – Stauffer et al. 1997; Allen et al. 2003). Reddening is small – $E(B - V) = 0.01$ mag (Randich et al. 2001) – and therefore negligible in the near-infrared (NIR) photometry reported here.

Patten & Simon (1996) published an impressive investigation of rotation, as revealed by star-spots, of cluster members with late spectral types (F8–M3): because of the youth of the cluster, this essentially provided information about rotation periods on the zero-age main-sequence, which is of interest in the context of the evolution of angular momentum (Stassun & Terndrup 2003). In the last few years there have been deliberate efforts to find very low-mass objects (VLMOs, i.e. stars or brown dwarfs) in IC 2391 – see Barrado y Navascués, Stauffer & Jayawardhana (2004), and references therein. The aim of the photometric observations reported here was to obtain rotation periods, as revealed by photometric variability, for a few of these VLMOs.

There has been considerable recent interest in studying the rotation properties of objects (stars and brown dwarfs) with masses below about $0.4 M_{\odot}$. Of course, one of the aims has been to research the mass dependence of rotation periods. Another focus area has been the time dependence of rotation rates: this has been investigated by measuring rotation periods in clusters or star forming regions of various ages – see e.g. Terndrup et al. (1999), Bailer-Jones & Mundt (2001), Eislöffel & Scholz (2002), Joergens et al. (2003),

Caballero et al. (2004), Scholz & Eislöffel (2004a,b), Lamm et al. (2005), and references therein. A useful summary of much of this work can be found in Scholz et al. (2005b).

A result which has emerged is that the mean rotation period decreases with decreasing mass, i.e. VLMOs are generally rapidly rotating. It also appears that the lower limit to rotation periods is independent of age: rapidly rotating VLMOs are seen in clusters with widely differing ages. Further investigation of these two points motivated the present study.

Our targets, with spectral types in the range M 5.5–M 7 were taken from Barrado y Navascués et al. (2004): salient information from that paper is reproduced in Table 1. These are the latest spectral types currently known in IC 2391, and their masses should be below $0.2 M_{\odot}$ (e.g. Leggett 1992). Data acquisition and manipulation are described in Section 2 below. Results of the photometry are given in Sections 3 (variability) and 4 (colour–magnitude and colour–colour diagrams). One of the new variables is discussed in more detail in Section 5. Conclusions follow in Section 6.

2 OBSERVATIONS AND REDUCTIONS

All observations were made with the SIRIUS camera attached to the 1.4-m Infrared Survey Facility (IRSF) telescope, situated at Sutherland, South Africa. The camera obtains simultaneous exposures in J , H and K_s of a 7.7×7.7 -arcmin² field, using three detectors. Further information about the instrument can be found in Nagayama et al. (2003).

Flat-field exposures were made twice, under clear evening conditions. Dark frames were obtained at the end of each night. Each time-series measurement was constructed from a dither pattern of 10 exposures. An integration time of 15 s per exposure was used throughout. Time resolution of a few minutes is adequate for studying variability on time-scales of hours: data acquisition was

★E-mail: ckoen@uwc.ac.za

Table 1. Target details.

Object name	Spectral type	J	H	K_s
CTIO-061	M 6.0	15.27	14.68	14.21
CTIO-062	M 6.0	14.95	14.39	13.99
CTIO-113	M 7.0	15.08	14.38	14.03
CTIO-136	M 5.5	14.13	13.48	13.13
CTIO-145	M 6.0	15.06	14.39	13.96
CTIO-160	M 7.0	15.12	14.47	14.10

Table 2. Observing log.

Starting time (HJD 2453390+)	Object names	Run length (h)	N
3.2776	CTIO-113, CTIO-145	6.9	54
4.3295	CTIO-062, CTIO-160	7.2	56
5.3210	CTIO-061, CTIO-136	7.6	59

therefore maximized by cycling between two fields. This enabled us to observe six fields in IC 2391, two on each of the three nights of good observing weather – see Table 2 for a log.

The initial stages of the reduction procedure – dark and flat-field corrections, sky estimation and subtraction – were performed with an IRAF-based pipeline. Profile magnitudes were calculated using an automated version of DOPHOT (Schechter, Mateo & Saha 1993). Software developed at SAAO was then used to assign consistent identifications for stars observed at different times or with different filters.

Differential magnitudes were calculated by selecting well observed ($N > 30$) local standards for each field. Generally, it was required that the scatter (s.d.) in the photometry of all comparison stars be less than 0.01 mag, but this had to be relaxed to 0.015 or 0.02 mag in a few instances to ensure that a good sample (more than 30) of standards be obtained.

Since the aim of the project was the study of variability, standardization of the photometry was not considered important. It is none the less useful to have some idea of the actual brightnesses of the stars. Crude magnitude zero-points were therefore set by comparing the mean magnitudes in J , H and K_s of the objects in Table 1 with the two-Micron All-Sky Survey (2MASS) (Cutri et al. 2003) photometry. Since two fields were observed contemporaneously, two zero-points could be determined for each night, for each of the filters. The averages of the two zero-points were then used to set the nightly zero-points.

3 VARIABLES

None of the targets showed convincing evidence for variability – see Fig. 1 for a plot of the J -band light curves. Standard deviation values of the sets of photometry varied between 0.005–0.007 mag (for the brightest object, CTIO-136) to 0.019–0.021 mag for CTIO-113. These values are completely in line with the scatter of other objects of similar brightness. Furthermore, no sign of any periodicity could be seen in the data.

It is tempting to look for reasons why no variability was seen in any of the six targets. Scholz, Eislöffel & Froebrich (2005a) showed that the modulation amplitude in VLMOs due to spots is expected to be smaller in the NIR than at optical wavelengths. Given that VLMO amplitudes are generally small even in the optical (Scholz

& Eislöffel 2004b), this could mean that variability is often below the NIR measurement threshold. Another possibility is that the time-scales involved are much longer than the single nights of monitoring in this project. However, rotation is expected, on average, to be very rapid in VLMOs (e.g. Scholz et al. 2005b), so that brightness changes on time-scales of several hours are not preposterous.

Another approach is to calculate the range of NIR detection probabilities compatible with the present null result. The 95 per cent confidence interval for p , the probability of finding variability, is [0, 0.4]. Conversely, even with $p = 0.4$ there would be a 5 per cent probability of finding no variables amongst six targets. For $p = 0.2$, the probability of a null result increases to 26 per cent. Perhaps we were just not lucky.

Observations of other stars in the fields were also scrutinized for variability. Photometry of many of the stars showed small systematic changes. That these were spurious could generally be seen from the fact that many data sets showed the same behaviour. (A brief discussion of these errors, and many example light curves, can be found in Koen, Matsunaga & Menzies 2004; the data discussed there were obtained with the same telescope and instrument as used in the project reported here). Unfortunately, this meant that automating the detection of variability was not trivial. Instead, we relied on the human eye. The light curve of each star with more than 15 measurements was examined, and photometry in all three filters of all candidate variables checked for confirmation.

Light curves of seven likely or obvious variables are shown in Figs 2–8. The J , H and K_s time-series are plotted on the same scales in order to demonstrate the wavelength dependence of the variations. Since the sensitivity of the instrument is not as good in K_s as in J and H , the two faintest objects could not always be measured in that waveband.

Approximate positions of the stars were found by comparison of finding charts generated from our photometry with the FK5 catalogue. These positions were then entered into the 2MASS point source catalogue (Cutri et al. 2003) in order to obtain the accurate positions (and 2MASS photometry) given in Table 3. None of these stars appears to have been specifically referred to in the astronomy literature.

Variables V2 and V4 are evidently eclipsing binaries, the former with a period very near to the run length (7.6 h). Variable 6 may also be a close binary – the last part of the light curves suggest a flat-bottomed eclipse. The period (1.43 h), light-curve shape and amplitude of V7 imply that it is a high-amplitude δ Scuti star: the decrease in amplitude with increasing wavelength confirms this. Although the period (3.03 h) of V1 is also consistent with its being a δ Scuti pulsator, the amplitude does not decrease with wavelength. The star may be a binary or perhaps a spotted rotator. The somewhat irregular appearance of the light curves argues in favour of the latter interpretation, whereas the wavelength independence of the amplitude is more consistent with the former hypothesis. If the star-spot explanation is correct, the very short rotation period would be of interest.

The low amplitudes of V3 and V5 place question marks over the identifications of these as variables. The increase of ‘flare’ amplitude with increasing wavelength in V3 is particularly unusual. We investigated the possibility that the brightness changes are artefacts, perhaps induced by seeing variations. However, no correlation could be found with either seeing or the brightnesses of nearby stars. Imperfect flat-fielding can of course be ruled out as very similar variations are seen in J and K brightnesses, which were measured on different detectors. The J and H variations in V5 appear roughly periodic, and closely similar frequencies of 7.8 d^{-1} ($P = 3.1 \text{ h}$) can

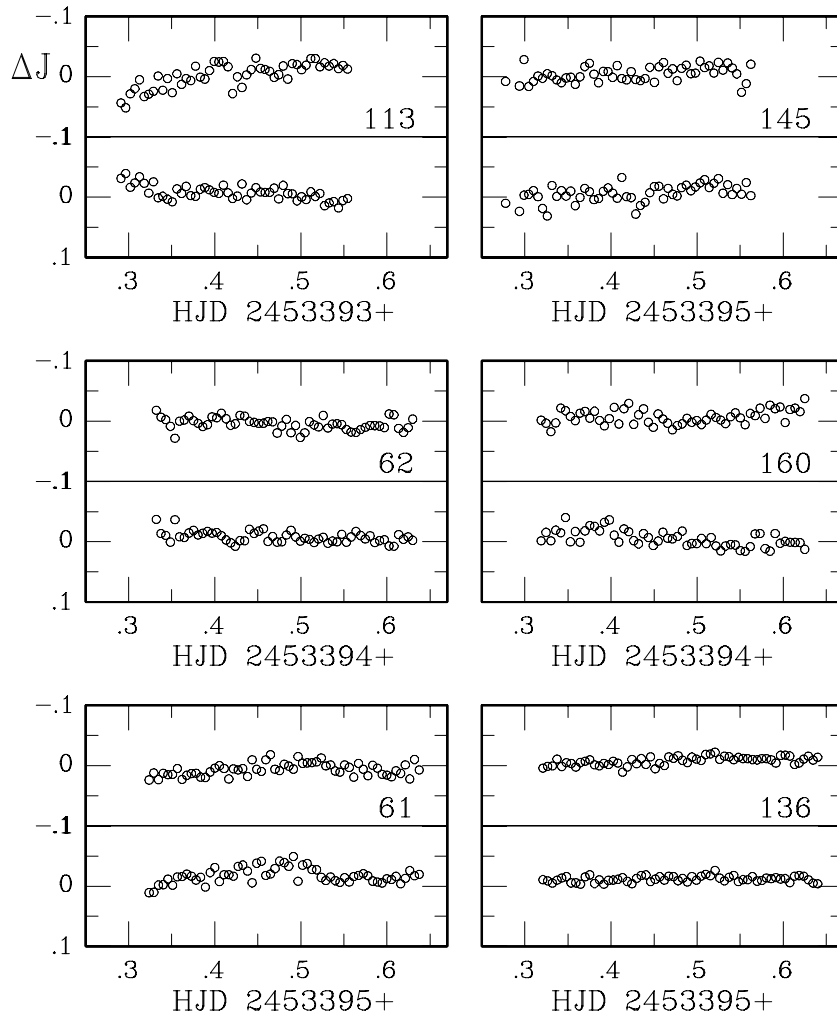


Figure 1. Light curves of the programme objects (top panels) and of stars of similar brightness from the same field (bottom panels), as measured through the *J* filter. The scales are the same on all panels; magnitude zero-points are arbitrary. Each group of two panels is labelled with the number from Table 1.

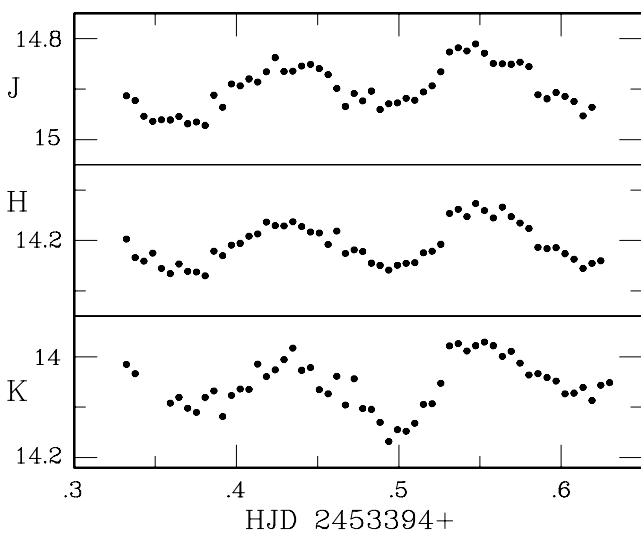


Figure 2. Light curves of variable 1 – see Table 3.

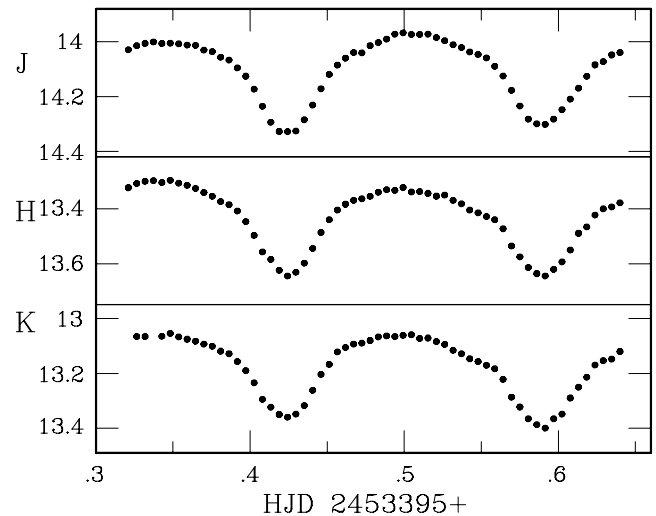


Figure 3. Light curves of variable 2 – see Table 3. This variable, which may be a cluster member, is discussed in more detail in Section 5.

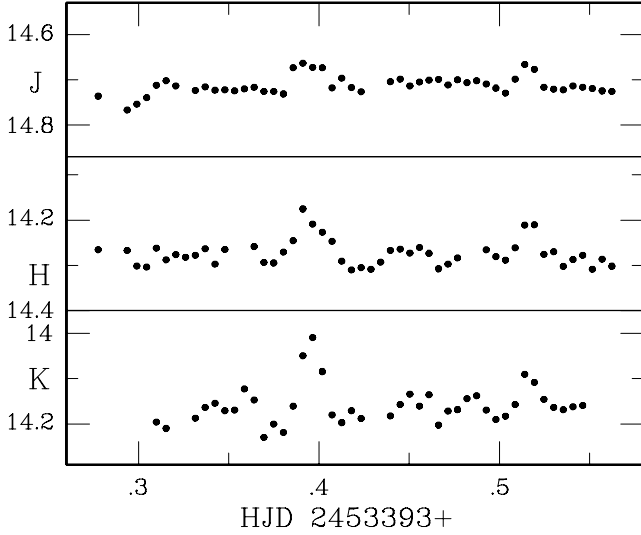


Figure 4. Light curves of variable 3 – see Table 3.

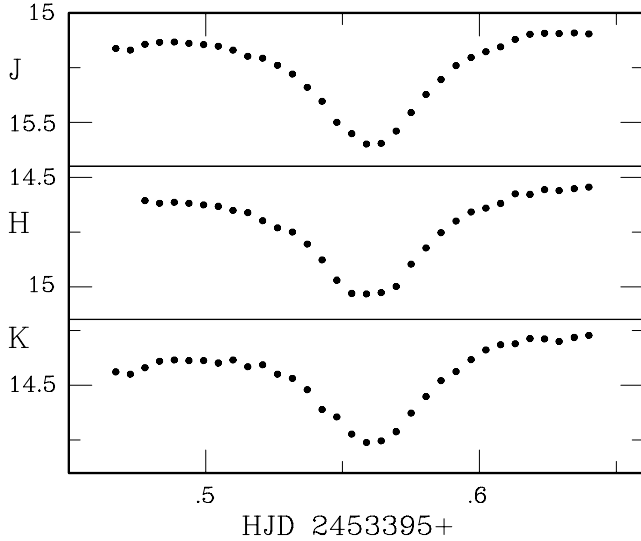


Figure 5. Light curves of variable 4 – see Table 3.

be extracted from both data sets. Similar variations may be present in K , but concealed by the greater noise level of the photometry.

Table 3 also shows colour indices calculated from our photometry, in order to allow the stars to be located in the diagrams given in the next section of the paper. It is noteworthy that V3 and V5 are amongst the bluest of all stars for which photometry was obtained: this is confirmed by their brightnesses in I , as given in the USNO-B1.0 catalogue. It is possible that the two stars are Be variables, although the authors are not aware that variability on such short time-scales has ever been seen in such objects.

Our average J magnitudes in Table 3 are consistently fainter than the 2MASS magnitudes, by typically about 0.1 mag. Since the zero-points were set by referring to very red stars, the implication is that there is a strong colour dependence in transforming between our J magnitudes and 2MASS J . There are also large (often several tenths of a magnitude) differences between our average H , K_s magnitudes and the 2MASS values, but the differences are not as systematic as in the case of the J filter.

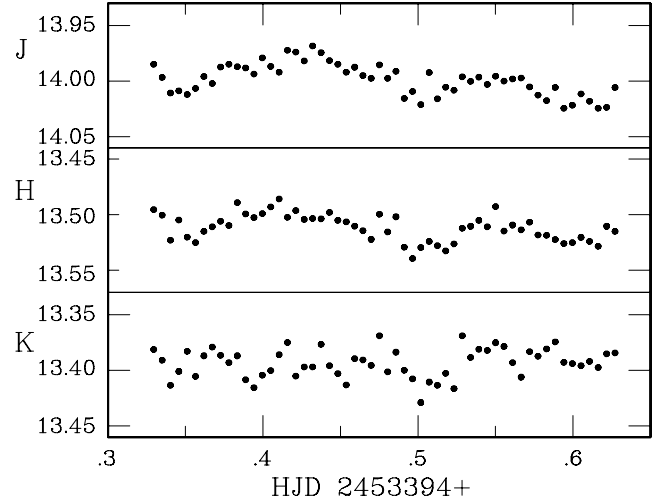


Figure 6. Light curves of variable 5 – see Table 3.

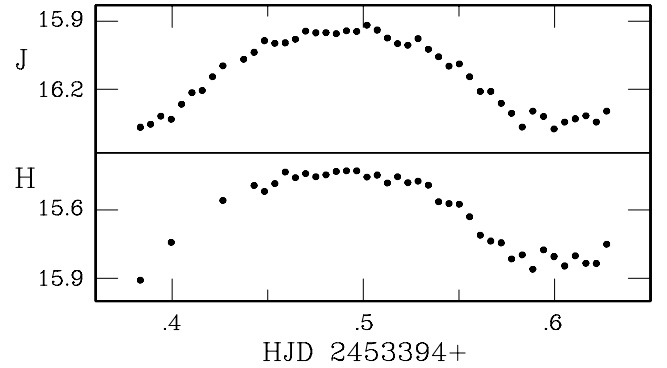


Figure 7. Light curves of variable 6 – see Table 3.

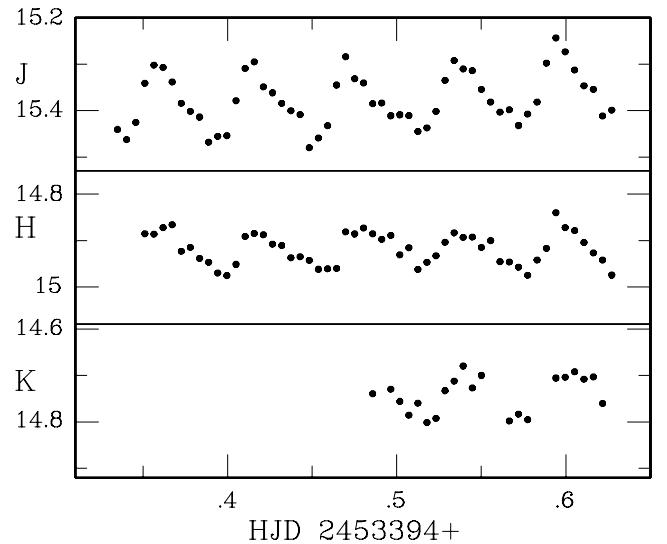


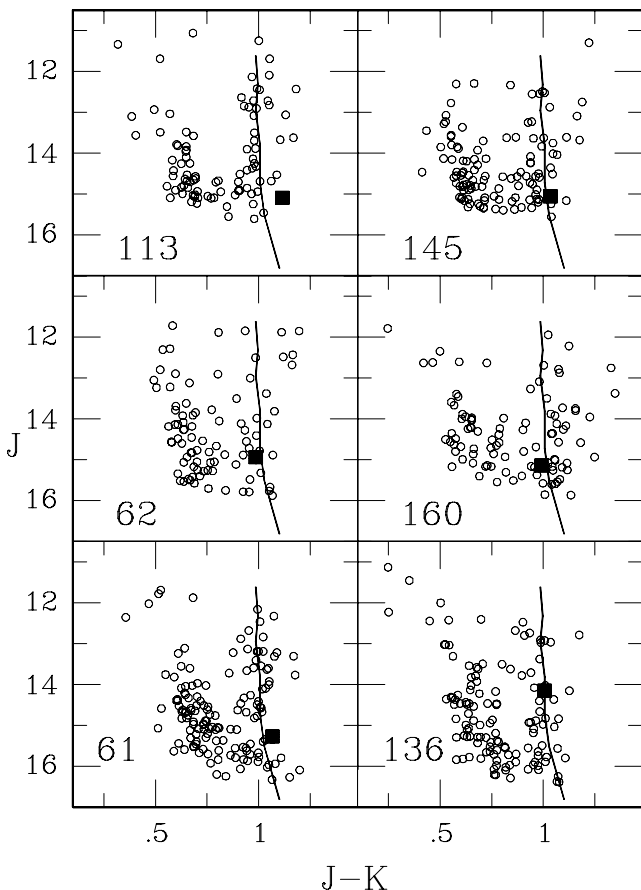
Figure 8. Light curves of variable 7 – see Table 3.

4 COLOUR-MAGNITUDE AND COLOUR-COLOUR DIAGRAMS

An advantage of our photometry is that stars were observed many times through each filter. This means that the errors in the

Table 3. New variable stars. Positions were taken from the 2MASS catalogue. The I magnitudes are from the USNO-B1.0 catalogue (Monet et al. 2003). Averages over all measurements through a given filter were used to calculate the photometry entered under ‘This paper’.

ID	Field	Position (2000)		2MASS photometry			This paper				
		Right ascension (RA)	Declination (Dec.)	J	H	K_s	J	$J - H$	$H - K_s$	$J - K_s$	I
V1	62	08:38:26.7	-52:45:06.6	14.74	14.12	13.92	14.90	0.69	0.15	0.84	15.41
V2	136	08:43:03.6	-52:56:12.8	13.90	13.26	13.19	14.10	0.67	0.25	0.92	14.82
V3	145	08:43:19.5	-53:12:46.3	14.60	14.17	14.15	14.71	0.44	0.11	0.55	15.12
V4	136	08:43:31.2	-52:55:01.7	15.26	14.84	14.65	15.25	0.53	0.27	0.80	16.14
V5	160	08:43:52.7	-52:43:48.9	13.28	12.89	12.86	14.00	0.49	0.12	0.61	13.09
V6	160	08:44:09.1	-52:45:37.2	15.90	15.37	15.56	16.14	0.53	-	-	17.05
V7	160	08:44:12.3	-52:46:18.7	15.28	14.99	14.93	15.38	0.46	0.18	0.64	16.03

**Figure 9.** Colour–magnitude plots for each of the six fields, based on accurately determined mean magnitudes. Data for the two fields observed during the same night are plotted next to each other. The lines denote the young disc lower main sequence from Leggett (1992). Solid squares denote the programme objects.

measurements can be estimated very reliably, which again allows us to select stars with accurate photometry for colour–magnitude and colour–colour plots. The plots below are based on average magnitudes, with the requirements of a minimum of 15 observations, and a maximum scatter of 0.03 mag, in each filter.

The $J - (J - K_s)$ colour–magnitude plots for the six fields can be seen in Fig. 9. These were calculated from the average magnitudes of each object. Data from fields sharing the same zero-points are plotted next to each other. The lower main sequence is visible near $J - K_s = 1$, running vertically (see espe-

cially the CTIO-113 data). For purposes of comparison the young disc lower main sequence from Leggett (1992) has been inserted, but it should be stressed that its location in Fig. 9 is uncertain. In theory the IRSF system is not so dissimilar from the CIT system used by Leggett (1992) (see http://www.z.phys.nagoya-u.ac.jp/sirius/about/color_e.html), but since the zero-points of our data are not well determined an additional shift of 0.12 mag in the transformed $J - K$ was made to give reasonable agreement between the two sequences.

A second sequence, also approximately vertical, is at bluer $J - K_s$ in Fig. 9: these stars are evidently background objects, which appear too faint for their colours as compared to the cluster members.

A glance at Fig. 9 shows that it is unlikely that any star bluer than $J - K_s = 0.8$ is a cluster member. This leaves V2 as the only strong membership contender from Table 3; the likelihood that V1 and/or V4 are members is lower. Variable V2 is therefore discussed in more detail in the next section of the paper.

In the case of V7 use can be made of the visual and K band period–luminosity relations to estimate absolute magnitudes and hence its distance. McNamara (2000) gives

$$M_V = -1.969 - 3.725 \log P \quad (1)$$

while unpublished work by Dr D. Laney (SAAO) leads to

$$M_K = -2.46 - 3.34 \log P. \quad (2)$$

Using the 2MASS K_s magnitude from Table 3 in (2), and the Guide Star Catalogue V magnitude of 16.99 in (1), distances of 4.57 (K_s) and 7.57 kpc (V) are obtained. Given the substantial (0.47 mag) uncertainty in the visual magnitude, the shorter distance is probably more realistic.

The $(J - H) - (H - K_s)$ colour–colour diagrams are plotted in Fig. 10. As in the case of Fig. 9, these were calculated from the average magnitudes of each object. In all cases but one the programme object (Table 1) is the reddest in the field in $H - K$. The exception is in the field of CTIO-136, where the programme object is the second reddest.

A few stars occupy positions in Fig. 10 similar to the programme stars of Table 1. Table 4 gives the details of these: one each was taken from the fields of CTIO-136 and CTIO-62, while five are from the field of CTIO-61. The last column of the table contains I magnitudes from the USNO-B1.0 catalogue: comparison of these with the J magnitudes shows that all the objects with the exception of C3 are very red and hence candidate very late-type stars. No unambiguous optical counterpart for C7 could be found, but it is the reddest in $H - K$ of all the stars in the study, and hence of some interest. The fact that C5 is substantially brighter than the other stars, despite having similar colours, suggests that it may be a foreground object.

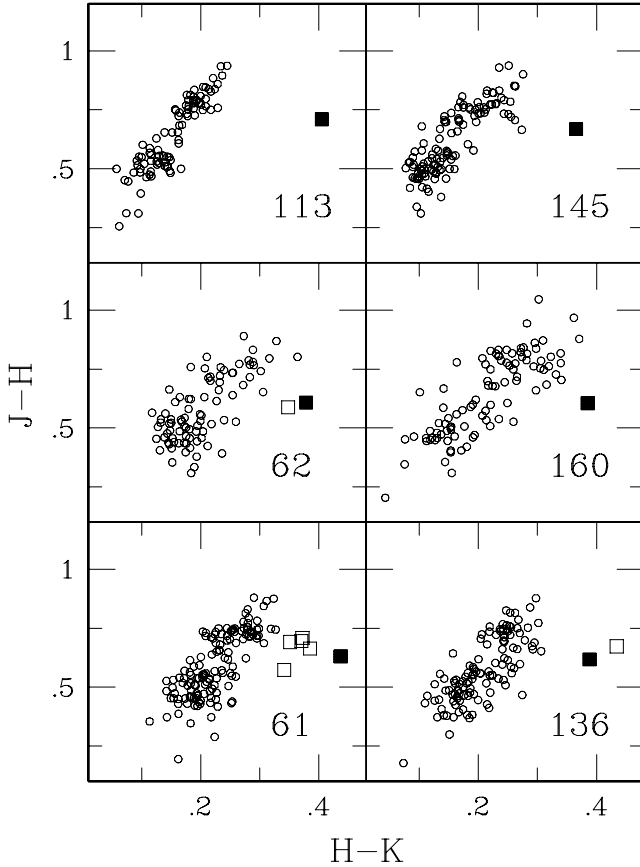


Figure 10. Colour–colour plots for each of the six fields, based on accurately determined mean magnitudes. Solid squares indicate the programme object, and open squares candidate VLMOs (see Table 4).

5 THE VARIABLE V2

If V2 is indeed a cluster member, then it is possible to deduce more about the star system. The absolute magnitude of the binary follows from the known distance modulus of 5.95 (Patten & Simon 1996) and the 2MASS magnitude as $M_J = 7.95$. It is clear from the light curves – in particular the similar depths of the two eclipses – that the two stars are of similar brightnesses. This means that $M_J \approx 8.7$ for either component. Leggett (1992) derived absolute magnitudes and infrared colours of M dwarfs: from her table 6, $M_J = 7.82, 8.73$ for young disc spectral types M4 and M5.5, respectively. Therefore, should it be a cluster member, V2 is unlikely to be of spectral type

earlier than M4. The more recent distance modulus derived by Dodd (2004) is only 0.1 mag brighter, hence the same conclusions would apply.

Inspection of the isochrones calculated by Baraffe et al. (1998) shows that at an age of 50 Myr, $M_J = 8.7$ corresponds to a star with $M = 0.1 M_\odot$ and $T_{\text{eff}} = 3060$ K. This mass implies a spectral type later than M4 (Leggett 1992; table 6), as does the temperature (e.g. Bessell 1979).

The point is of some importance because of the scarcity of eclipsing binaries composed of two M dwarfs – see e.g. Ribas (2003), Maceroni & Montalbán (2004) and Creevey et al. (2005). Further observations and/or detailed modelling are required to establish the exact nature of V2. Below we only report on simple calculations based mainly on the light-curve shapes.

The continuously variable light curves, almost equal eclipse depths and short period imply that V2 is a W UMa binary. As pointed out by Rucinski (1993), the overall shapes of W UMa type light curves are largely determined by only three parameters: the mass ratio, orbital inclination and the degree of contact (see Rucinski 1973 for a formal definition of the latter). Furthermore, the values of these parameters can be estimated from observed light curves. This is conveniently done by approximating the suitably normalized and phased intensity light curve $I = I(\phi)$ by a finite cosine series

$$I(\phi) \approx \sum_{k=0}^{10} a_k \cos(2\pi k\phi)$$

and comparing the cosine coefficients to values tabulated by Rucinski (1993). Only a_2, a_4 and a_6 are important. Values of these three coefficients were determined by least squares for each of the three light curves, and are displayed in Table 5. The agreement between the three sets of numbers is very good. Comparison with fig. 6 in Rucinski (1993) shows that the (a_2, a_4) pairs lie very slightly above the zero contact line, suggesting marginal non-contact.

The eclipse depths are $\Delta I = 0.27\text{--}0.28$: scrutiny of table 4 in Rucinski (1993) shows that this implies an orbital inclination angle close to 68 degrees, and a mass ratio $0.4 \leq q \leq 0.6$.

Using a period $P = 0.327$ d (double the time interval between the two eclipses), it follows from Kepler’s law,

$$A^3 = G(M_1 + M_2) \left(\frac{P}{2\pi} \right)^2,$$

that the separation between the two stars is $2m^{1/3} R_\odot$, where m is the total system mass, in solar units. Given the near-contact configuration, i.e. both stars almost filling their Roche lobes, radii considerably larger than those usually associated with mid-M dwarfs

Table 4. Candidate very cool objects. Positions were taken from the 2MASS catalogue. Averages over all measurements through a given filter were used to calculate the photometry entered under ‘This paper’. The last column contains the I magnitudes from the USNO-B1.0 catalogue (Monet et al. 2003). No optical counterpart for C7 could be found within 3 arcsec of the 2MASS position; counterparts for other stars were all within 0.75 arcsec.

ID	Field	Position (2000)		2MASS photometry			This paper				
		RA	Dec.	J	H	K_s	J	$J - H$	$H - K_s$	$J - K_s$	I
C1	61	08:38:39.0	−52:12:20.8	16.03	15.44	15.22	16.02	0.69	0.35	1.04	17.38
C2	61	08:38:43.5	−52:11:38.4	16.33	15.24	15.09	16.33	0.70	0.37	1.07	17.84
C3	61	08:38:47.1	−52:11:30.2	15.46	14.89	14.91	15.94	0.71	0.37	1.08	15.32
C4	61	08:38:54.7	−52:12:10.0	15.92	15.19	14.97	15.96	0.66	0.39	1.05	17.32
C5	62	08:39:09.4	−52:42:20.1	11.78	11.22	10.93	11.85	0.59	0.35	0.94	13.35
C6	61	08:39:10.1	−52:12:40.8	14.35	13.89	13.61	14.46	0.57	0.34	0.91	15.54
C7	136	08:43:33.6	−52:59:54.5	15.80	15.05	14.76	15.80	0.67	0.43	1.11	–

Table 5. Selected cosine coefficients derived from the light curves of the eclipsing binary V2. Standard errors are given in brackets.

Filter	a_2	a_4	a_6
<i>J</i>	$-1.17E-1$ (2.2E-3)	$-3.5E-2$ (2.2E-3)	$-1.5E-2$ (2.3E-3)
<i>H</i>	$-1.15E-1$ (2.0E-3)	$-3.0E-2$ (2.0E-3)	$-1.5E-2$ (2.0E-3)
<i>K_s</i>	$-1.12E-1$ (1.8E-3)	$-3.2E-2$ (1.8E-3)	$-1.5E-2$ (1.8E-3)

are implied. In fact, the Baraffe et al. (1998) model of a 50-Myr-old object with $M = 0.1 M_{\odot}$ gives $\log g = 4.72$, which translates to a radius of $0.23 R_{\odot}$. This suggests that V2 may be a background object.

We also note in passing that the position of one of the 99 X-ray sources in IC 2391 discovered by Marino et al. (2005), is within 1 arcsec of V2.

6 CONCLUSIONS

Perhaps the most useful positive results produced by this study has been the new variable stars in Table 3, and the very red stars in Table 4. The unusual variable V3 (and possibly V5) seem particularly worthy of further study. The increase in variability amplitude with wavelength implies that the star is redder when it is brighter. This, together with its very blue average colour, suggest that it is a Be star (e.g. de Wit et al. 2003). If this speculation is correct, then the rapid flaring is interesting.

Unfortunately, our null result for variability in the target objects does not allow us to set very stringent limits on detection of NIR variability in such objects (at noise levels similar to ours): the 95 per cent confidence interval for the detection probability is [0, 0.4], based on the six non-detections. The results can also be compared with those of Barrado y Navascués, Huéllamo & Calderón (2005): the authors found *J*-band variability in three very low-mass targets in a field in the λ Orionis cluster, from several hours of time-series photometry during one night.

ACKNOWLEDGMENTS

Use of the Simbad data base, the US Naval Observatory B1.0 catalogue, the Guide Star Catalogue, and the 2MASS point source catalogue, are gratefully acknowledged. We are also grateful to Drs. Motohide Tamura and Dave Laney for helpful comments, and to Dr Y. Nakajima (Department of Astrophysics, Nagoya University), for use of his IRAF-based pipeline for the reduction of SIRIUS observations. The referee's comments prompted improvement of the paper.

IRAF is distributed by the National Optical Astronomy Observatories, which is operated by the Association of Universities for Research in Astronomy, Inc., under contract to the National Science Foundation, USA.

REFERENCES

- Allen P. R., Trilling D. E., Koerner D. W., Reid I. N., 2003, *ApJ*, 595, 1222
 Bailer-Jones C. A. L., Mundt R., 2001, *A&A*, 367, 218
 Baraffe I., Chabrier G., Allard F., Hauschildt P. H., 1998, *A&A*, 337, 403
 Barrado y Navascués D., Stauffer J. R., Patten B. M., 1999, *ApJ*, 522, L56
 Barrado y Navascués D., Stauffer J. R., Jayawardhana R., 2004, *ApJ*, 614, 386
 Barrado y Navascués D., Huéllamo N., Calderón M. M., 2005, *Astron. Nachr.*, 326, 981
 Bessell M., 1979, *PASP*, 91, 589
 Caballero J. A., Béjar V. J. S., Rebolo R., Zapatero Osorio M. R., 2004, *A&A*, 424, 857
 Creevey O. L. et al., 2005, *ApJ*, 625, L127
 Cutri R. M. et al., 2003, 2MASS All-Sky Catalog of Point Sources, CDS/ADC Electronic Catalogues, 2246
 de Wit W. J., Beaulieu J.-P., Lamers H. J. G. L. M., Lesquoy E., Marquette J.-B., 2003, *A&A*, 410, 199
 Dodd R. J., 2004, *MNRAS*, 355, 959
 Eislöffel J., Scholz A., 2002, in Alves J. F., McCaughrean M. J., eds, *The Origins of Stars and Planets: The VLT View*. Springer-Verlag, Berlin, p. 219
 Joergens V., Fernández M., Carpenter J. M., Neuhäuser R., 2003, *ApJ*, 594, 971
 Koen C., Matsunaga N., Menzies J., 2004, *MNRAS*, 354, 466
 Lamm M. H., Mundt R., Bailer-Jones C. A. L., Herbst W., 2005, *A&A*, 430, 1005
 Leggett S. K., 1992, *ApJS*, 82, 351
 Maceroni C., Montalbán J., 2004, *A&A*, 426, 577
 Marino A., Micela G., Peres G., Pillitteri I., Sciortino S., 2005, *A&A*, 430, 287
 McNamara D. H., 2000, in Breger M., Montgomery M. H., eds, *ASP Conf. Ser. Vol. 210, Delta Scuti and Related Stars*. Astron. Soc. Pac., San Francisco, p. 373
 Monet D. G., Levine S. E., Casian B. et al., 2003, *AJ*, 125, 984
 Nagayama T. et al., 2003, *Proc. SPIE*, 4841, 459
 Patten B. M., Simon T., 1996, *ApJS*, 106, 489
 Randich S., Pallavicini R., Meola G., Stauffer J. R., Balachandran S. C., 2001, *A&A*, 372, 862
 Ribas I., 2003, *A&A*, 398, 239
 Rucinski S. M., 1973, *Acta Astron.*, 23, 79
 Rucinski S. M., 1993, *PASP*, 105, 1433
 Schechter P. L., Mateo M., Saha A., 1993, *PASP*, 105, 1342
 Scholz A., Eislöffel J., 2004a, *A&A*, 419, 249
 Scholz A., Eislöffel J., 2004b, *A&A*, 421, 259
 Scholz A., Eislöffel J., Froebrich D., 2005a, *A&A*, 438, 675
 Scholz A., Jayawardhana R., Eislöffel J., Froebrich D., 2005b, *Astron. Nachr.*, 326, 895
 Stassun K. G., Terndrup D., 2003, *PASP*, 115, 505
 Stauffer J. R., Hartmann L. W., Prosser C. F., Randich S., Balachandran S., Patten B. M., Simon T., Giampapa M., 1997, *ApJ*, 479, 776
 Terndrup D. M., Krishnamurthi A., Pinsonneault M. H., Stauffer J. R., 1999, *AJ*, 118, 1814

This paper has been typeset from a $\text{\TeX}/\text{\LaTeX}$ file prepared by the author.